Geophys. J. Int. (2009) doi: 10.1111/j.1365-246X.2009.04230.x

Surface-wave sensitivity to 3-D anelasticity

Ying Zhou

Department of Geosciences, Virginia Tech, Blacksburg, VA 24061, *USA. E-mail: yingz@vt.edu*

Accepted 2009 April 24. Received 2009 April 20; in original form 2009 January 26

SUMMARY

Lateral variations in mantle anelasticity (Q) are important for understanding the Earth's thermal and chemical structure in the mantle. In the past decades, preliminary global 3-D tomographic Q models have been developed based upon the assumption that traveltime (phase delay) anomalies are due to the Earth's elastic (velocity) structure whereas amplitude anomalies are dominated by 3-D anelastic (Q) structure. In this paper, we calculate the 3-D finite-frequency sensitivity of fundamental-mode surface-wave phase delays and amplitudes to perturbations in anelasticity (Q). Calculations of Q and velocity sensitivity kernels show that (1) roughly 15–20 per cent of observed phase delays in long-period surface waves can be explained by lateral variations in Q in the upper mantle; and (2) focusing and defocusing effects due to 3-D velocity structure account for a major portion of observed amplitude perturbations in long-period surface waves. The coupling between elastic and anelastic effects in both seismic traveltimes and amplitudes indicates that a joint inversion of 3-D velocity and 3-D Q structure accounting for both anelastic dispersion and associated focusing and defocusing effects is necessary in mapping lateral heterogeneities in the upper mantle.

Key words: Surface waves and free oscillations; Seismic attenuation; Seismic tomography; Theoretical seismology; Wave scattering and diffraction.

1 INTRODUCTION

It has been long recognized that the Earth is not purely elastic, and seismic energy loss caused by the Earth's internal frictions can be characterized by the seismic quality factor, Q. The anelasticity (Q) can be explained by a thermally activated mechanism, leading to strong dependence of Q upon temperature variations. This makes the Earth's anelastic (Q) structure valuable in resolving thermal and compositional origins of seismic anomalies in the mantle. Despite of their great importance, studies of the Earth's anelasticity structure have progressed only slowly in the past decades: global Q models are in general less well resolved compared to velocity models, and large discrepancies exist among global Q models (e.g. Romanowicz 1995; Romanowicz & Durek 2000; Selby & Woodhouse 2002; Romanowicz 2003; Dalton & Ekström 2006).

The effects of anelasticity (Q) on seismic waves are twofold: (1) amplitude attenuation—amplitudes of seismic waves decay with propagation distance due to energy loss and (2) anelastic dispersion—wave propagation speed varies with frequency due to the relaxation of stress and strain. In global anelasticity (Q) tomography, amplitudes have been considered in constructing 3-D Q models, and the effects of anelastic dispersion due to 3-D Q structure have been ignored (e.g. Billien *et al.* 2000; Selby & Woodhouse 2002; Gung & Romanowicz 2004; Dalton & Ekström 2006).

The importance of anelastic dispersion was first recognized in the 1970s when radial (1-D) variations in seismic attenuation (Q) were proposed to explain the discrepancy between velocity models inverted using long-period normal mode data and short-period body wave data. Several 1-D (radial) Q models have been developed and the radial structure of Q has been incorporated in many global surface-wave tomographic studies (e.g. Anderson & Hart 1978; Dziewonski & Anderson 1981; Widmer *et al.* 1991; Durek & Ekström 1996). In contrast, the effects of anelastic dispersion due to lateral variations in Q (3-D Q structure) have received very limited attention.

In global surface-wave tomography, the most widely used observables are frequency-dependent phase-delay and amplitude measurements. Up to date, global upper-mantle 3-D Q structure are mainly obtained using the amplitude information of surface waves. It is known that amplitudes are sensitive not only to 3-D Q structure but also sensitive to 3-D wave speed structure due to focusing and defocusing of seismic waves. For this reason, amplitudes can be potentially used to provide constraints on wave speed structure complementary to phase-delay data (e.g. Woodhouse & Wong 1986; Laske & Masters 1996; Zhou *et al.* 2004). However, the relative importance of 3-D Q and 3-D velocity structure in surface-wave amplitudes have not been well understood.

In the past decades, efforts have been made to overcome the resolution limit of ray theory in surface-wave tomography (e.g. Snieder & Nolet 1987; Romanowicz 1987; Marquering *et al.* 1998; Spetzler *et al.* 2002; Zhou *et al.* 2004; Yoshizawa & Kennett 2005; Tromp *et al.* 2005;

Dahlen & Zhou 2006; Liu & Tromp 2008) and the majority of the work have been focused on surface-wave sensitivity to perturbations in seismic velocity. In this paper, we derive finite-frequency surface-wave sensitivity kernels of *both* phase delays and amplitudes to perturbations in anelasticity (Q), and we point out that in the upper mantle: (1) 3-D Q structure affects not only the amplitude of surface waves, but also significantly the phase delay (traveltime) of surface waves; and, (2) 3-D velocity structure (focusing/defocusing) accounts for a major portion of observed amplitude perturbations in long-period surface waves.

2 3-D VELOCITY KERNELS

We briefly review the surface-wave Born theory of Zhou *et al.* (2004). For simplicity, we consider only single-frequency, fundamental-mode, surface-wave sensitivity to perturbations in S- and P-wave speeds (β and α). The effect of applying either a single or multiple tapers in measurement processes can be accounted for using the procedures described in sections 4 and 9 of Zhou *et al.* (2004).

In the presence of lateral heterogeneities, ground displacement response to a moment tensor source can be written as $u(\omega) + \delta u(\omega)$, where $u(\omega)$ represents the vertical, radial or transverse component of the displacement in the reference earth model, and $\delta u(\omega)$ represents the perturbation in displacement due to perturbations in S- and P-wave speeds and can be written as (Zhou *et al.* 2004),

$$\delta u(\omega) = \iiint_{\oplus} \left[\mathcal{K}^{\beta} \left(\frac{\delta \beta}{\beta} \right) + \mathcal{K}^{\alpha} \left(\frac{\delta \alpha}{\alpha} \right) \right] d^3\mathbf{x}, \tag{1}$$

where $\mathcal{K}^{\beta}(\omega, \mathbf{x})$ and $\mathcal{K}^{\alpha}(\omega, \mathbf{x})$ are the complex waveform kernels (Zhou *et al.* 2004). To the first order, phase delays and amplitude perturbations of single-frequency surface waves can be written as (Zhou *et al.* 2004)

$$\delta\phi(\omega) = -\mathrm{Im}\left(\frac{\delta u}{u} \right), \qquad \delta \ln A(\omega) = \mathrm{Re}\left(\frac{\delta u}{u} \right). \tag{2}$$

In the single-scattering (Born) approximation, phase delay $\delta\phi(\omega)$ and amplitude perturbation $\delta \ln A\ (\omega)$ can be expressed as volumetric integrations of fractional perturbations in S- and P-wave speeds,

$$\begin{aligned} \delta\phi(\omega) &= \iiint_{\oplus} \left[K_{\phi}^{\beta} \left(\frac{\delta \beta}{\beta} \right) + K_{\phi}^{\alpha} \left(\frac{\delta \alpha}{\alpha} \right) \right] d^3\mathbf{x}, \\ \delta \ln A(\omega) &= \iiint_{\oplus} \left[K_{A}^{\beta} \left(\frac{\delta \beta}{\beta} \right) + K_{A}^{\alpha} \left(\frac{\delta \alpha}{\alpha} \right) \right] d^3\mathbf{x}, \end{aligned} \tag{3}$$

where $K_{\phi}^{\beta}(\omega, \mathbf{x}) = -\mathrm{Im}[\mathcal{K}^{\beta}(\omega, \mathbf{x})/u(\omega)]$ and $K_{A}^{\beta}(\omega, \mathbf{x}) = \mathrm{Re}[\mathcal{K}^{\beta}(\omega, \mathbf{x})/u(\omega)]$ are the corresponding phase and amplitude velocity kernels (Zhou *et al.* 2004).

3 3-D Q KERNELS—PHASE AND AMPLITUDE

Following Zhou *et al.* (2004), we consider a spherically symmetric reference earth model in which density, elastic moduli as well as anelasticity (quality factors Q_{μ} and Q_{κ}) depend only on the radius (or depth). This reference earth model is then subjected to perturbations in the inverse of the quality factors,

$$Q_{\mu}^{-1} \to Q_{\mu}^{-1} + \delta Q_{\mu}^{-1}, \qquad Q_{\kappa}^{-1} \to Q_{\kappa}^{-1} + \delta Q_{\kappa}^{-1}. \tag{4}$$

Local perturbations in anelasticity can be incorporated using complex elastic moduli μ and κ (Dahlen & Tromp 1999, section 9), yielding,

$$\begin{aligned} \frac{\delta\mu}{\mu} &= \left[i\delta Q_{\mu}^{-1} + \frac{2}{\pi} \delta Q_{\mu}^{-1} \ln\left(\frac{\omega}{\omega_0} \right) \right] \left[1 + i\, Q_{\mu}^{-1} + \frac{2}{\pi} Q_{\mu}^{-1} \ln\left(\frac{\omega}{\omega_0} \right) \right] \\ \frac{\delta\kappa}{\kappa} &= \left[i\delta Q_{\kappa}^{-1} + \frac{2}{\pi} \delta Q_{\kappa}^{-1} \ln\left(\frac{\omega}{\omega_0} \right) \right] \left[1 + i\, Q_{\kappa}^{-1} + \frac{2}{\pi} Q_{\kappa}^{-1} \ln\left(\frac{\omega}{\omega_0} \right) \right], \end{aligned} \tag{5}$$

where ω_0 is the reference frequency of the velocity model and ω is the frequency of the seismic wave. In the mantle, Q values are relatively large and we make the following first-order approximation,

$$1 + i\, Q_{\mu}^{-1} + \frac{2}{\pi} Q_{\mu}^{-1} \ln\left(\frac{\omega}{\omega_0} \right) \approx 1, \quad 1 + i\, Q_{\kappa}^{-1} + \frac{2}{\pi} Q_{\kappa}^{-1} \ln\left(\frac{\omega}{\omega_0} \right) \approx 1, \tag{6}$$

and the fractional perturbations in the complex moduli in eq. (5) can be written as

$$\begin{aligned} \frac{\delta\mu}{\mu} &= \left[i\delta Q_{\mu}^{-1} + \frac{2}{\pi} \delta Q_{\mu}^{-1} \ln\left(\frac{\omega}{\omega_0} \right) \right], \\ \frac{\delta\kappa}{\kappa} &= \left[i\delta Q_{\kappa}^{-1} + \frac{2}{\pi} \delta Q_{\kappa}^{-1} \ln\left(\frac{\omega}{\omega_0} \right) \right]. \end{aligned} \tag{7}$$

The imaginary part in eq. (7) leads to perturbations in amplitudes, and the real part results in frequency-dependent perturbations in wave speeds, i.e. 3-D anelastic dispersion.

To the first order, perturbations in elastic moduli can be related to perturbations in *P*- and *S*-wave speeds,

$$\frac{\delta\alpha}{\alpha} = \frac{1}{2}\left[(1-\gamma)\frac{\delta\kappa}{\kappa} + \gamma\frac{\delta\mu}{\mu} - \frac{\delta\rho}{\rho}\right],$$
$$\frac{\delta\beta}{\beta} = \frac{1}{2}\left[\frac{\delta\mu}{\mu} - \frac{\delta\rho}{\rho}\right], \qquad \text{where } \gamma = \frac{4}{3}\frac{\beta^2}{\alpha^2}, \tag{8}$$

and $\delta\rho/\rho = 0$ for purely anelastic perturbations. Upon substituting eqs (7) and (8) into eqs (1) and (2), phase delays and amplitude perturbations can be written as volumetric integrations of fractional perturbations in Q_μ^{-1} and Q_κ^{-1},

$$\delta\phi(\omega) = \iiint_\oplus \left[K_\phi^{Q_\mu}\left(\frac{\delta Q_\mu^{-1}}{Q_\mu^{-1}}\right) + K_\phi^{Q_\kappa}\left(\frac{\delta Q_\kappa^{-1}}{Q_\kappa^{-1}}\right)\right] d^3\mathbf{x},$$
$$\delta \ln A(\omega) = \iiint_\oplus \left[K_A^{Q_\mu}\left(\frac{\delta Q_\mu^{-1}}{Q_\mu^{-1}}\right) + K_A^{Q_\kappa}\left(\frac{\delta Q_\kappa^{-1}}{Q_\kappa^{-1}}\right)\right] d^3\mathbf{x}, \tag{9}$$

where $K_\phi^{Q_\mu}(\omega, \mathbf{x})$ and $K_\phi^{Q_\kappa}(\omega, \mathbf{x})$ are the phase-delay Q kernels—representing the sensitivity of surface-wave phase delays to fractional perturbations in Q_μ^{-1} and Q_κ^{-1}; and $K_A^{Q_\mu}(\omega, \mathbf{x})$ and $K_A^{Q_\kappa}(\omega, \mathbf{x})$ are the amplitude Q kernels—representing the sensitivity of surface-wave amplitudes to fractional perturbations in Q_μ^{-1} and Q_κ^{-1}. The Q kernels in eq. (9) are related to the velocity kernels in eq. (3) by

$$K_\phi^{Q_\mu} = -\frac{1}{2Q_\mu}(K_A^\beta + \gamma K_A^\alpha) + \frac{1}{\pi Q_\mu}(K_\phi^\beta + \gamma K_\phi^\alpha)\ln\left(\frac{\omega}{\omega_0}\right),$$
$$K_A^{Q_\mu} = \frac{1}{2Q_\mu}(K_\phi^\beta + \gamma K_\phi^\alpha) + \frac{1}{\pi Q_\mu}(K_A^\beta + \gamma K_A^\alpha)\ln\left(\frac{\omega}{\omega_0}\right),$$
$$K_\phi^{Q_\kappa} = -\frac{1}{2Q_\kappa}(1-\gamma)K_A^\alpha + \frac{1}{\pi Q_\kappa}(1-\gamma)K_\phi^\alpha\ln\left(\frac{\omega}{\omega_0}\right),$$
$$K_A^{Q_\kappa} = \frac{1}{2Q_\kappa}(1-\gamma)K_\phi^\alpha + \frac{1}{\pi Q_\kappa}(1-\gamma)K_A^\alpha\ln\left(\frac{\omega}{\omega_0}\right). \tag{10}$$

Where the terms associated with the natural logarithm of the frequency are a result of anelastic dispersion. In general, the Earth's anelastic effects on bulk modulus are much smaller than that on shear modulus, i.e. $Q_\mu \ll Q_\kappa$; as a result, surface-wave sensitivity to perturbations in Q_κ^{-1}($K_\phi^{Q_\kappa}$ and $K_A^{Q_\kappa}$) is much weaker than the sensitivity to perturbations in Q_μ^{-1}($K_\phi^{Q_\mu}$ and $K_A^{Q_\mu}$). For fundamental-mode Love waves, $K_\phi^\alpha = K_A^\alpha = 0$ and $K_\phi^{Q_\kappa} = K_A^{Q_\kappa} = 0$.

The amplitude kernels $K_A^{Q_\mu}$ and $K_A^{Q_\kappa}$ have been discussed in Dahlen & Zhou (2006) where the second terms in $K_A^{Q_\mu}$ and $K_A^{Q_\kappa}$ in eq. (10)—representing the focusing and defocusing due to 3-D anelastic dispersion—have been neglected. There are two main differences between Dahlen & Zhou (2006) and this study: (1) sensitivity kernels in Dahlen & Zhou (2006) were formulated for purely elastic reference earth models, i.e. $Q_\mu^{-1} = Q_\kappa^{-1} = 0$. In this paper, sensitivity kernels are formulated for reference earth models with radial variations in Q; and (2) only amplitude kernels were derived in Dahlen & Zhou (2006) with considerations limited to the imaginary part of the perturbations in the complex moduli in eq. (7). Therefore, focusing and defocusing effects due to 3-D anelastic dispersion were not accounted for. In this paper, sensitivity kernels are formulated for both amplitude perturbations and phase delays, fully accounting for wave attenuation as well as anelastic dispersion.

4 KERNEL EXAMPLES

Fig. 1 shows examples of phase-delay and amplitude Q kernels $K_\phi^{Q_\mu}$ and $K_A^{Q_\mu}$ as well as velocity kernels K_ϕ^β and K_A^β, all computed for a Love wave at a period of 100 s. The reference earth model is PREM (Dziewonski & Anderson 1981) at a reference period of 1 s. The Q kernels and velocity kernels are very similar in geometry, but their polarities are the opposite. This is because (1) unlike *S*-wave velocity, an increase in Q^{-1} (decrease in Q) will slow down surface waves and lead to an increase in phase delay; and (2) the focusing and defocusing terms (second terms in eq. 10) dominate the phase and amplitude Q kernel $K_\phi^{Q_\mu}$ and $K_A^{Q_\mu}$ at 100 s. Examples of sensitivity kernels $K_{\phi,A}^{Q_\mu}$ and $K_{\phi,A}^\beta$ for a 100-s Rayleigh wave are plotted in Fig. 2.

In Figs 1 and 2, the Q kernels and velocity kernels are plotted on different colour scales. The velocity phase-delay kernels are about 50 times stronger than the Q phase-delay kernels, i.e. $|K_\phi^\beta| \approx 50 \times |K_\phi^{Q_\mu}|$; and the velocity amplitude kernels are about 80 times stronger than the Q amplitude kernels, i.e. $|K_A^\beta| \approx 80 \times |K_A^{Q_\mu}|$. The Q sensitivity kernels reach their maximum in the low Q region in PREM at depths between 80 and 220 km. It is worth pointing out that lateral variations in Q in the upper mantle are about 10 times stronger than lateral variations in *S*-wave velocity, with *S*-wave velocity perturbations in the order of ±6 per cent and perturbations in Q_μ^{-1} in the order of ±60 per cent (e.g. Romanowicz 1995; Selby & Woodhouse 2000; Zhou *et al.* 2006; Dalton *et al.* 2008). Based upon the magnitude of K_ϕ^β and $K_\phi^{Q_\mu}$ as well as the strength of seismic anomalies in velocity and anelasticity in the upper mantle, surface-wave phase delays at 100-s caused by 3-D velocity structure are predicted to be roughly five times of the delay times caused by 3-D Q structure. This is consistent with phase-delay measurements made on synthetic seismograms generated using the Spectral Element Method (Komatitsch & Tromp 1999) for global 3-D

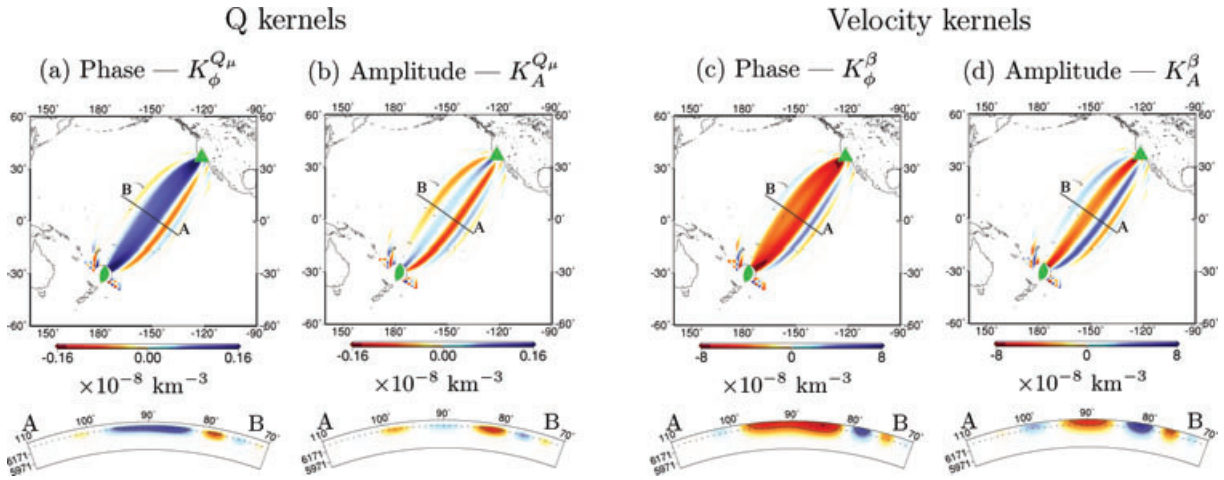

Figure 1. (a) and (b) are Q kernels $K_\phi^{Q_\mu}$ and $K_A^{Q_\mu}$—representing the sensitivity of phase delay and amplitude to fractional perturbations in Q_μ^{-1}; (c) and (d) are velocity kernels K_ϕ^{β} and K_A^{β}—representing the sensitivity of phase delay and amplitude to fractional perturbations in S-wave speed β. All sensitivity kernels are computed for a 100-s Love wave and all mapviews are plotted at a depth of 100 km. The reference earth model is PREM at a reference period of 1 s.

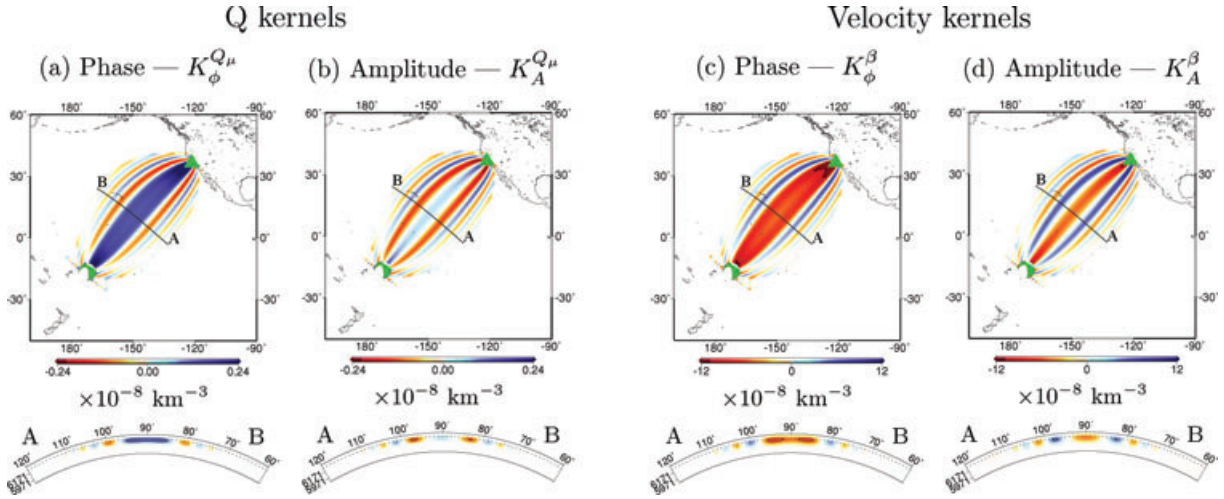

Figure 2. The same as Fig. 1 but for a 100-s Rayleigh wave.

velocity and 3-D Q models (Ruan & Zhou 2008), about 15–20 per cent of observed long-period surface-wave phase delays can be explained by the 3-D Q structure in the upper mantle.

As pointed by Zhou *et al.* (2004), surface-wave amplitudes are more sensitive to the geometry of the anomalies in the mantle due to their more oscillatory sensitivity in space. In Section 7, we show that in the limit of ray theory, amplitudes are sensitive to the second spatial derivative ('roughness') of perturbations in velocity and anelasticity. The relative importance of 3-D velocity structure and 3-D Q structure in surface-wave amplitudes depends upon both the magnitude of the sensitivity kernels ($K_A^{\beta,\alpha}$ and $K_A^{Q_\mu,Q_\kappa}$) and the 'roughness' of the anomalies in velocity and anelasticity. The 'roughness' (second spatial derivatives) of mantle anomalies in velocity and anelasticity are not well resolved in present-day tomographic studies. If the origin of the upper-mantle heterogeneities is dominantly thermal, the average 'roughness' of Q anomalies in the upper mantle is unlikely to be more than ∼80 times larger than that of velocity anomalies (Ruan & Zhou 2008), therefore, surface-wave amplitude perturbations are dominated by the focusing and defocusing effects introduced by 3-D velocity structure. It is important to point out this conclusion is drawn based upon reference earth models with a reasonable radial (1-D) Q structure such as PREM. It is known that surface-wave amplitudes can differ greatly between seismograms generated in a purely elastic 1-D earth model and an earth model with a reasonable radial Q structure. However, lateral variations (3-D) in Q do not contribute to amplitudes as much as lateral (3-D) variations in velocity structure.

It is worth noting that the fact amplitude perturbations are dominated by focusing and defocusing effects does not necessarily indicate current Q tomographic models have been overestimated. This is because (1) inaccuracy in tomographic theory will introduce internal inconsistency in the inverse system, which often requires greater damping to be applied in the inversion; (2) focusing and defocusing effects have been treated differently in different Q tomographic studies; whereas large discrepancies exist among global Q models developed by

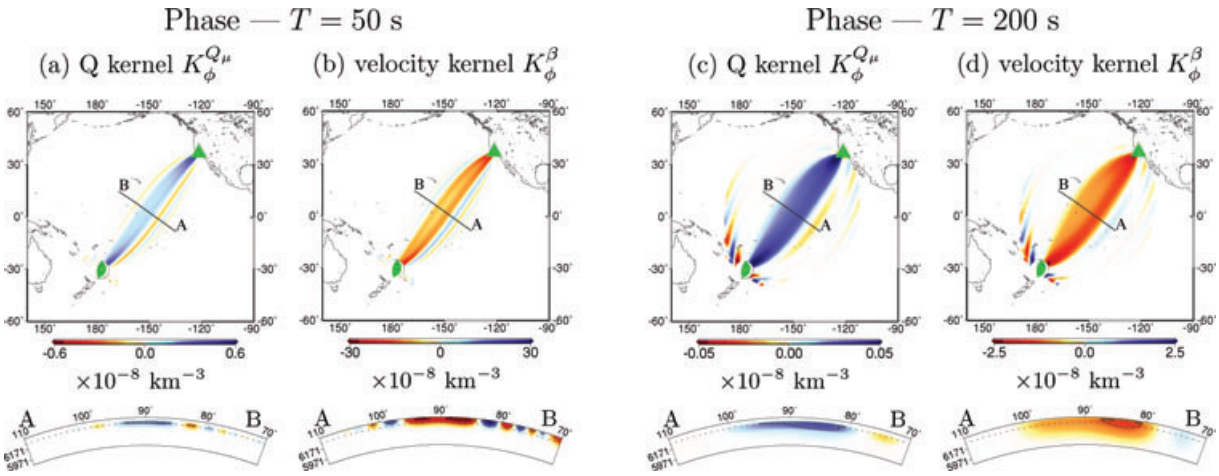

Figure 3. Phase-delay kernels $K_\phi^{Q_\mu}$ and K_ϕ^β computed for Love waves at 50 s (a and b) and 200 s (c and d).

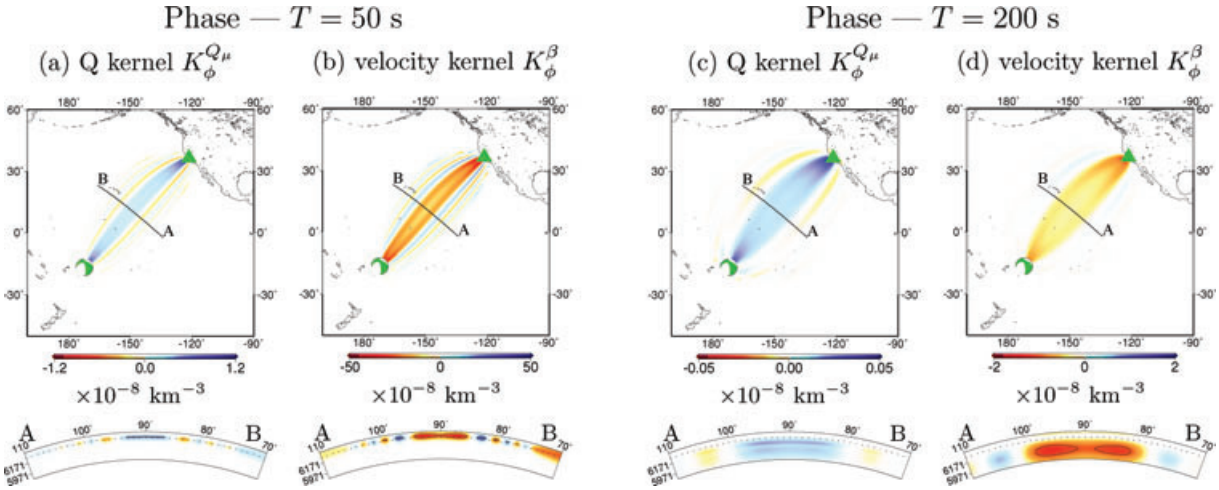

Figure 4. The same as Fig. 4 but for 50-s and 200-s Rayleigh waves.

different research groups, the amplitudes of the models are all comparable (e.g. Gung & Romanowicz 2004; Dalton *et al.* 2008). In this paper, we have assumed that current global velocity and Q models are correct in order of magnitude.

5 FREQUENCY DEPENDENCE

Phase-delay and amplitude Q sensitivity kernels are dependent upon the frequency of surface waves. Fig. 3 shows examples of phase-delay sensitivity kernels to perturbations in Q_μ^{-1} and S-wave speed β for 50-s (a and b) and 200-second (c and d) Love waves. Examples of Rayleigh-wave sensitivity kernels at 50 s and 200 s are plotted in Fig. 4. As expected, both velocity kernels and Q kernels show deeper and wider sensitivity at longer periods. The Q kernels and velocity kernels are plotted on different colour scales—the scales for velocity kernels are 50 times of the scales for Q kernels. The ratios of $|K_\phi^\beta|/|K_\phi^{Q_\mu}|$ and $|K_A^\beta|/|K_A^{Q_\mu}|$ for the maximum along-ray sensitivity half-way between the source and the receiver are plotted in Fig. 5 for Love waves (blue lines) and Rayleigh waves (red lines) as a function of wave period. Overall, the relative importance of 3-D Q structure in surface-wave phase delays (or amplitudes) increases with the period of the surface wave, and, perturbations in Q have more significant effects on Rayleigh waves than on Love waves at the same period. For example, for Love waves, $|K_\phi^\beta|/|K_\phi^{Q_\mu}| \approx 90$ at 50 s $|K_\phi^\beta|/|K_\phi^{Q_\mu}| \approx 40$ at 200 s; and the ratios become $|K_\phi^\beta|/|K_\phi^{Q_\mu}| \approx 45$ and $|K_\phi^\beta|/|K_\phi^{Q_\mu}| \approx 38$ for Rayleigh waves at 50 and 200 s, respectively.

6 REDUCTION TO 2-D KERNELS

In this section, we show that the 3-D Q kernels in eq. (9) for fundamental-mode surface-wave phase delays and amplitudes can be reduced to 2-D sensitivity to perturbations in the inverse of the local surface-wave quality factor Q^{-1} ($Q_{\rm L}^{-1}$ for Love waves and $Q_{\rm R}^{-1}$ for Rayleigh waves). Following a similar approach of Zhou *et al.* (2004), we make a forward-scattering approximation (scatter angle $\eta = 0$), the anelastic analogue

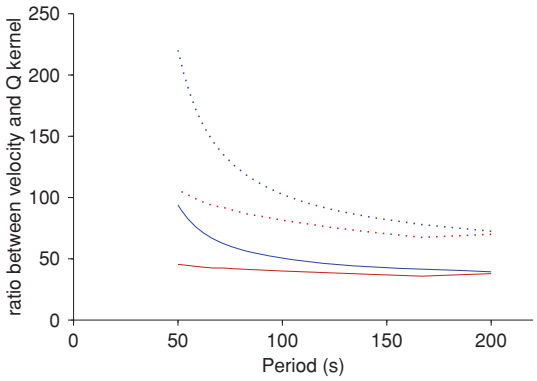

Figure 5. Ratios of $|K_\phi^\beta|/|K_\phi^{Q_\mu}|$ (solid line) and $|K_A^\beta|/|K_A^{Q_\mu}|$ (dotted line) of the maximum along-ray sensitivity half way between the source and the receiver plotted as a function of wave period from 50 to 200 s: blue lines, Love waves; red lines, Rayleigh waves. Source-receiver configurations are as the same as in Figs 3 and 4.

of eq. (6.2) of Zhou *et al.* (2004) becomes

$$\int_0^a \left[(1-\gamma)\Omega^\alpha \delta Q_\kappa^{-1} + (\Omega^\beta + \gamma\Omega^\alpha)\delta Q_\mu^{-1}\right] r^2 dr = \frac{-2\omega^2}{cC}\delta Q^{-1}, \tag{11}$$

where c and C are the local phase velocity and group velocity in the reference earth model, both measured in rad s^{-1} on the unit sphere; and Q^{-1} is the inverse of the local surface-wave quality factor (Dahlen & Tromp 1999, section 9),

$$Q^{-1} = \frac{cC}{-2\omega^2}\int_0^a \left[(1-\gamma)\Omega^\alpha Q_\kappa^{-1} + (\Omega^\beta + \gamma\Omega^\alpha)Q_\mu^{-1}\right] r^2\, dr, \tag{12}$$

where Ω^α and Ω^β are the surface-wave scattering coefficients as given in the appendix of Zhou *et al.* (2004) with the scattering angle being $\eta = 0$.

Upon substituting eqs (10) and (11) into eq. (9), the phase delay and amplitude perturbations can be written as a 2-D integral of fractional perturbations in the inverse of the local surface-wave (Love-wave or Rayleigh-wave) quality factor,

$$\delta\phi(\omega) = \iint_\Omega K_\phi^Q(\hat{\mathbf{r}}, \omega)\left(\frac{\delta Q^{-1}}{Q^{-1}}\right) d\Omega, \qquad \delta \ln A(\omega) = \iint_\Omega K_A^Q(\hat{\mathbf{r}}, \omega)\left(\frac{\delta Q^{-1}}{Q^{-1}}\right) d\Omega, \tag{13}$$

and the integrations are over the unit sphere $\Omega = \{\hat{\mathbf{r}} : ||\hat{\mathbf{r}}||^2 = 1\}$. The 2-D Q kernels $K_{\phi,A}^Q(\hat{\mathbf{r}}, \omega)$ are related to the 2-D phase-velocity kernels $K_{\phi,A}^c(\hat{\mathbf{r}}, \omega)$ of Zhou *et al.* (2004) by

$$K_\phi^Q = \frac{c}{2CQ}\left[\frac{2}{\pi}\ln\left(\frac{\omega}{\omega_0}\right)K_\phi^c - K_A^c\right], \qquad K_A^Q = \frac{c}{2CQ}\left[K_\phi^c + \frac{2}{\pi}\ln\left(\frac{\omega}{\omega_0}\right)K_A^c\right]. \tag{14}$$

It is worth-noting that both K_ϕ^Q and K_A^Q are combinations of K_ϕ^c and K_A^c. For model PREM at a reference period of 1 s, the leading terms in K_ϕ^Q and K_A^Q in eq. (14) are the terms associated the natural logarithm of the frequency ($\ln(\omega/\omega_0)$) for long-period (50–200 s) surface waves.

7 REDUCTION TO RAY THEORY

We show that the 2-D Q sensitivity kernels in eqs (13) and (14) can be further reduced to ray theory in the limit of infinite frequency based upon a paraxial, forward-scattering approximation as applied in Zhou *et al.* (2004) for velocity kernels.

7.1 Phase-delay kernels

The 2-D phase-delay sensitivity kernels in eq. (13) can be simplified by making a paraxial, forward-scattering approximation (Zhou *et al.* 2004), and the phase delay can be written as

$$\delta\phi = \frac{\omega^2}{cCQ}\iint_\Omega \sqrt{\frac{\Gamma}{8\pi k}}\left[-\frac{2}{\pi}\ln\left(\frac{\omega}{\omega_0}\right)\sin\left(\frac{1}{2}k\Gamma y^2 + \frac{\pi}{4}\right) + \cos\left(\frac{1}{2}k\Gamma y^2 + \frac{\pi}{4}\right)\right]\frac{\delta Q^{-1}}{Q^{-1}} d\Omega, \tag{15}$$

where $\Gamma = \sin\Delta/[\sin x\, \sin(\Delta - x)$, with Δ being the epicentral distance and x being the along ray path distance. We make a zeroth-order expansion $\delta Q^{-1}(x, y) \approx \delta Q^{-1}(x, 0)$ in the integration of the first term in eq. (15) and a second-order expansion $\delta Q^{-1}(x, y) \approx \delta Q^{-1}(x, 0) + y\partial_y \delta Q^{-1}(x, 0) + (1/2)\, y^2\partial_y^2 \delta Q^{-1}(x, 0)$ in the integration of the second term, the local perturbation in Q^{-1} can be extracted from the cross-path integral in eq. (15), and the phase delay can be expressed as a 1-D integral along the geometrical ray path,

$$\delta\phi = \frac{-\omega}{\pi CQ}\ln\left(\frac{\omega}{\omega_0}\right)\int_0^\Delta \frac{\delta Q^{-1}}{Q^{-1}}\, dx - \frac{c}{4CQ\sin\Delta}\int_0^\Delta \sin x\, \sin(\Delta - x)\partial_y^2\frac{\delta Q^{-1}}{Q^{-1}}\, dx. \tag{16}$$

For model PREM at a reference period of 1 second, surface-wave phase delays at 100 s are about 400 times more sensitive to fractional perturbations in Q^{-1} than to the second spatial derivatives of the perturbation field. For anomalies with a characteristic length scale comparable to the wavelength of the 100-s surface waves (∼400 km), the magnitude of $\partial_y^2 \delta Q^{-1}/Q^{-1}$ is about 250 times stronger than $\delta Q^{-1}/Q^{-1}$. This indicates that phase delays due to 3-D perturbations in anelasticity is dominated by the perturbation field $\delta Q^{-1}/Q^{-1}$ rather than the second derivative of the perturbation field.

Considering phase delays due to both elastic model perturbations as well as anelastic perturbations, the total ray-theoretical phase delay can be written as

$$\delta\phi = \delta\phi_{\rm el} + \delta\phi_{\rm an} = -k\int_0^\Delta \frac{\delta c}{c}dx - \frac{\omega}{\pi C Q}\ln\left(\frac{\omega}{\omega_0}\right)\int_0^\Delta \frac{\delta Q^{-1}}{Q^{-1}}dx - \frac{c}{4CQ\sin\Delta}\int_0^\Delta \sin x\sin(\Delta - x)\partial_y^2\frac{\delta Q^{-1}}{Q^{-1}}dx, \tag{17}$$

where the first term is the elastic phase delay term, eq. (7.7) of Zhou *et al.* (2004), which was first derived using a strictly ray-theoretical argument by Woodhouse & Wong (1986).

7.2 Amplitude kernels

The 2-D amplitude sensitivity kernels in eq. (13) can also be simplified using the paraxial, forward-scattering approximation, yielding,

$$\delta\ln A = -\frac{\omega^2}{cCQ}\iint_\Omega \sqrt{\frac{\Gamma}{8\pi k}}\left[\sin\left(\frac{1}{2}k\Gamma y^2 + \frac{\pi}{4}\right) + \frac{2}{\pi}\ln\left(\frac{\omega}{\omega_0}\right)\cos\left(\frac{1}{2}k\Gamma y^2 + \frac{\pi}{4}\right)\right]\frac{\delta Q^{-1}}{Q^{-1}}d\Omega. \tag{18}$$

Upon making a zeroth-order and a second-order expansion on δQ^{-1} in the integration of the first term and the second term in eq. (18), respectively, amplitude perturbations due to fractional perturbations in Q^{-1} reduce to a 1-D integral along the geometrical ray path,

$$\delta\ln A = -\frac{\omega}{2CQ}\int_0^\Delta \frac{\delta Q^{-1}}{Q^{-1}}dx + \frac{c}{2\pi CQ\sin\Delta}\ln\left(\frac{\omega}{\omega_0}\right)\int_0^\Delta \sin x\sin(\Delta - x)\partial_y^2\frac{\delta Q^{-1}}{Q^{-1}}dx, \tag{19}$$

where the first term is the ray-theoretical amplitude attenuation (energy loss) term, and the second term is the focusing and defocusing term associated with anelastic dispersion. For model PREM at a reference period of 1 s, the ray-theoretical sensitivity of 100-s surface-wave amplitudes to $\delta Q^{-1}/Q^{-1}$ is roughly 60 times stronger than the sensitivity to $\partial_y^2\delta Q^{-1}/Q^{-1}$. For anomalies with a characteristic length scale comparable to the wavelength of the 100-s surface waves (∼400 km), the magnitude of $\partial_y^2\delta Q^{-1}/Q^{-1}$ is about 250 times stronger than $\delta Q^{-1}/Q^{-1}$. It indicates that long-period surface-wave amplitudes due to 3-D perturbations in anelasticity is dominated by the second derivative of the perturbation field. This is consistent with the geometry of the velocity and Q sensitivity kernels in Figs 1 and 2: the amplitude (velocity or Q) kernels are more oscillatory in space than the phase-delay (velocity or Q) kernels.

Considering amplitude perturbations due to both elastic model perturbations as well as anelastic perturbations, the total ray-theoretical amplitude perturbations can be written as

$$\delta\ln A = -\frac{1}{2\sin\Delta}\int_0^\Delta \sin x\sin(\Delta - x)\partial_y^2\frac{\delta c}{c}dx - \frac{\omega}{2CQ}\int_0^\Delta \frac{\delta Q^{-1}}{Q^{-1}}dx + \frac{c}{2\pi CQ\sin\Delta}\ln\left(\frac{\omega}{\omega_0}\right)\int_0^\Delta \sin x\sin(\Delta - x)\partial_y^2\frac{\delta Q^{-1}}{Q^{-1}}dx, \tag{20}$$

where the first term is the elastic focusing and defocusing term, eq. (7.12) of Zhou *et al.* (2004), which was first derived using a strictly ray-theoretical argument by Woodhouse & Wong (1986). For model PREM at a reference period of 1 s, the ray-theoretical sensitivity of 100-s surface-wave amplitudes to $\partial_y^2\delta c/c$ is about 80 times larger than the sensitivity to $\partial_y^2\delta Q^{-1}/Q^{-1}$. This is consistent with the ratio between the magnitude of the 3-D sensitivity kernels $|K_A^\beta|/|K_A^{Q_\mu}|$ as shown in Fig. 5. The ray-theoretical sensitivity confirms that long-period surface-wave amplitudes are more sensitive to the focusing and defocusing caused by 3-D elastic perturbations than to lateral (3-D) variations in anelasticity.

8 CONCLUSIONS

We derive surface-wave phase-delay and amplitude sensitivity kernels to fractional perturbations in anelasticity (Q_κ^{-1} and Q_μ^{-1}); the phase-delay kernels account for 3-D anelastic dispersion effects and the amplitude kernels account for both amplitude attenuation (energy loss) and the focusing and defocusing effects caused by 3-D anelastic dispersion. Comparisons between Q sensitivity kernels and velocity sensitivity kernels show that (1) upper-mantle 3-D Q structure have significant effects on surface-wave phase delays: roughly 15–20 per cent of observed long-period surface-wave phase delays can be explained by the 3-D Q structure in the upper mantle; surface-wave tomographic results can be biased if 3-D anelastic dispersion effects are not correctly accounted for; (2) When the reference earth model has a reasonable radial Q structure (such as PREM), focusing and defocusing effects due to 3-D velocity structure in the upper mantle account for a major portion of observed amplitude perturbations in long-period surface waves.

The fact that elastic and anelastic effects are coupled in seismic amplitudes has been appreciated in several pioneering studies where both phase-delay and amplitude data have been used in joint inversions of elastic and anelastic structures (e.g. Billien *et al.* 2000; Dalton & Ekström 2006). The limitations of those global studies are (1) the effects of 3-D anelastic dispersion have been neglected in those studies; (2) focusing and defocusing effects associated with 3-D anelastic dispersion have not been accounted for; and (3) upper-mantle velocity and Q structures have been jointed inverted based upon seismic ray theory, which breaks down whenever the length scale of the heterogeneity is comparable to (or smaller than) the characteristic wavelength of the seismic waves. The finite-frequency surface-wave sensitivity kernels developed in this paper opens the opportunity for joint diffractional tomography of 3-D velocity and 3-D Q structure in the upper mantle, fully accounting for both anelastic dispersion and the associated focusing and defocusing effects.

ACKNOWLEDGMENTS

I wish to thank the Editor Jeannot Trampert and the two reviewers, Anne Sieminski and an anonymous reviewer, for their thoughtful and constructive comments that significantly improved the manuscript. This research was financially supported by the US National Science Foundation under Grant EAR-0809464. All maps were generated using the Generic Mapping Tools (GMT; Wessel & Smith 1995).

REFERENCES

Anderson, D.L. & Hart, R.S., 1978. *Q* of the Earth, *J. geophys. Res.,* **83,** 5869–5882.

Billien, M., Lèvêque, J.-J. & Trampert, J., 2000. Global maps of Rayleigh wave attenuation for periods between 40 and 150 seconds, *Geophys. Res. Lett.,* **27,** 3619–3622.

Dahlen, F.A. & Tromp, J., 1998. *Theoretical Global Seismology*, Princeton University Press, Princeton, NJ.

Dahlen, F.A. & Zhou, Y., 2006. Surface-wave group-delay and attenuation kernels, *Geophys. J. Int.,* **165,** 545–554.

Dalton, C.A. & Ekström, G., 2006. Global models of surface wave attenuation, *J. geophys. Res.,* **111,** doi:10.1029/2005JB003997.

Dalton, C.A., Ekström, G. & Dziewonski, A.M., 2008. Global models of surface wave attenuation, *J. geophys. Res.,* **111,** B05317, doi:10.1029/2005JB003997.

Durek, J.J. & Ekström, G., 1996. A radial model of anelasticity consistent with long-period surface-wave attenuation, *Bull. seism. Soc. Am.,* **86,** 144–158.

Dziewonski, A.M. & Anderson, D.L., 1981. Preliminary reference Earth Model, *Phys. Earth planet. Int.,* **25,** 297–356.

Gung, Y. & Romanowicz, B., 2004. *Q* tomography of the upper mantle using three-component long-period waveforms, *Geophys. J. Int.*, doi:10.1111/j.1365-246X.2004.02135.x.

Komatitsch, D. & Tromp, J., 1999. Introduction to the spectral-element method for 3-D seismic wave propagation, *Geophys. J. Int.,* **139,** 806–822.

Laske, G. & Masters, G., 1996. Constraints on global phase velocity maps from long-period polarization data, *J. geophys. Res.,* **101,** 16 059–16 075.

Liu, Q. & Tromp, J., 2008. Finite-frequency sensitivity kernels for global seismic wave propagation based upon adjoint methods, *Geophys. J. Int.,* **174,** 265–286.

Marquering, H., Nolet, G. & Dahlen, F.A., 1998. Three-dimensional waveform sensitivity kernels, *Geophys. J. Int.,* **132,** 521–534.

Romanowicz, B., 1987. Multiplet–multiplet coupling due to lateral heterogeneity: asymptotic effects on the amplitude and frequency of the Earth's normal modes, *Geophys. J. R. astr. Soc.,* **90,** 75–100.

Romanowicz, B., 1995. A global tomographic model of shear attenuation in the upper mantle, *J. geophys. Res.,* **100,** 12 375–12 394.

Romanowicz, B., 2003. Global mantle tomography: Progress status in the past 10 years, *Annu. Rev. Earth Planet. Sci.,* **31,** 303–328.

Romanowicz, B. & Durek, J.J., 2000. Seismological constraints on attenuation in the Earth: a review, *Earths deep interior. Mineral Physics and Tomography from the Atomic to the Global Scale (AGU)*, 161–179.

Ruan, Y. & Zhou, Y., 2008. The effects of 3-D Q structure on surface wave phase delay. *Eos trans*. AGU, **89**(53), Fall Meet. Suppl., Abstract DI31B-1802.

Selby, N.D. & Woodhouse, J.H., 2000. Controls on Rayleigh wave amplitudes: attenuation and focusing, *Geophys. J. Int.,* **142,** 933–940.

Selby, N.D. & Woodhouse, J.H., 2002. The *Q* structure of the upper mantle: constraints from Rayleigh wave amplitudes, *J. geophys. Res.,* **107,** doi:10.1029/2001JB000257.

Snieder, R. & Nolet, G., 1987. Linearized scattering of surface waves on a spherical Earth, *J. geophys.* **61,** 55–63.

Spetzler, J., Trampert, J. & Snieder, R., 2002. The effects of scattering in surface wave tomography, *Geophys. J. Int.,* **149,** 755–767.

Tromp, J., Tape, C. & Liu, Q., 2005. Seismic tomography, adjoint methods, time reversal and banana-doughnut kernels, *Geophys. J. Int.,* **160,** 195–216.

Wessel, P. & Smith, W.H.F., 1995. New version of the Generic Mapping Tools released, *EOS trans.,* **76,** 329.

Widmer, R., Masters, G. & Gilbert, F., 1991. Spherically symmetric attenuation within the Earth from normal mode data. *Geophys. J. Int.,* **104,** 541–553.

Woodhouse, J.H. & Wong, Y.K., 1986. Amplitudes, phase and path anomalies of mantle waves, *Geophys. J. R. astr. Soc.,* **87,** 753–773.

Yoshizawa, K. & Kennett, B.L. N., 2005. Sensitivity kernels for finite-frequency surface waves, *Geophys. J. Int.,* **162,** 910–926.

Zhou, Y., Dahlen, F.A. & Nolet, G., 2004. 3-D sensitivity kernels for surface-wave observables, *Geophys. J. Int.,* **158,** 142–168.

Zhou, Y., Nolet, G., Dahlen, F.A. & Laske, G., 2006. Global upper-mantle structure from finite-frequency surface-wave tomography, *J. geophys. Res.,* **111,** doi:10.1029/2005JB003677.